COMPARISON BETWEEN ELECTRONIC HOT SPOT MODEL AND CURRENT-VOLTAGE CHARACTERISTICS OF SUPERCONDUCTING HOT-ELECTRON BOLOMETERS

D. Wilms Floet[1ab], J.R. Gao[2], T.M. Klapwijk[1], and P.A.J. de Korte[2]

[1]*Department of Applied Physics, Delft University of Technology, Lorentzweg 1, 2628 CJ Delft, The Netherlands*

[2]*Space Research Organization of the Netherlands, 9700 AV Groningen, The Netherlands*

Abstract

We compare theoretical predictions based on the electronic hot spot (EHS) model for hot electron bolometers with experimental results obtained with a Nb diffusion-cooled bolometer. We calculate the current-voltage, I(V), characteristics both analytically and numerically and find a good agreement with unpumped and pumped experimental I(V) curves. Observed deviations can partially be explained by the thermal conductance of the superconducting parts of the microbridge, which is lower than the normal state value assumed in the analytical model. Remaining deviations are attributed to heat-trapping due to Andreev reflection, resulting in a thermal boundary resistance at the interface. Furthermore, the influence of a finite electron-electron interaction time, which prevents complete thermalization of the electrons, is discussed.

I. Introduction

Despite the rapid progress in HEB mixer development from the experimental side, it is not fully clear yet what the limits of their performance are. This question has been a central subject of several studies, in which the bolometer, being essentially a superconducting microbridge contacted by normal conducting banks, is treated as a so-called transition-edge detector (lumped element approach) [1,2]. In these papers a broken-line transition model represents the resistive transition of the microbridge. Recently, however, the authors have shown that the resistive transition of the HEB of the microbridge is only relevant at a bath temperature close to the critical temperature T_c of the microbridge [3].

At low bath temperatures, where the actual mixing experiments are being performed, the lumped element approach is no longer adequate and the presence of a temperature profile in the microbridge has to be taken into account. We have proposed to describe heterodyne operation of the HEB mixer in terms of an electronic hot spot (EHS)

[a] Corresponding address: University of Groningen, Department of Applied Physics, Nijenborgh 4, 9747 AG Groningen, The Netherlands

[b] Electronic mail: wilms@phys.rug.nl

of which the length, and consequently the resistance, oscillates at the intermediate frequency[4,5]. This process is schematically depicted in Fig. 1. The potential importance of hot spot formation in phonon-cooled HEB mixers was also recognized in [6]. From a different perspective others have recently taken into account the temperature profile in the microbridge, but continue to relate the mixing properties to a local temperature dependent resistance [7,8]. In our EHS model, it is the *length of the resistor* that changes.

In this paper we compare analytical and numerical predictions made by the EHS-model with experimental results obtained on a Nb HEB mixer. We will mainly focus on the pumped and unpumped I(V) characteristics. In Section II we discuss the heat balance equations which we use to calculate the I(V) curves of the device. In Section III we present measurements of the pumped I(V) characteristics of the Nb HEB and compare

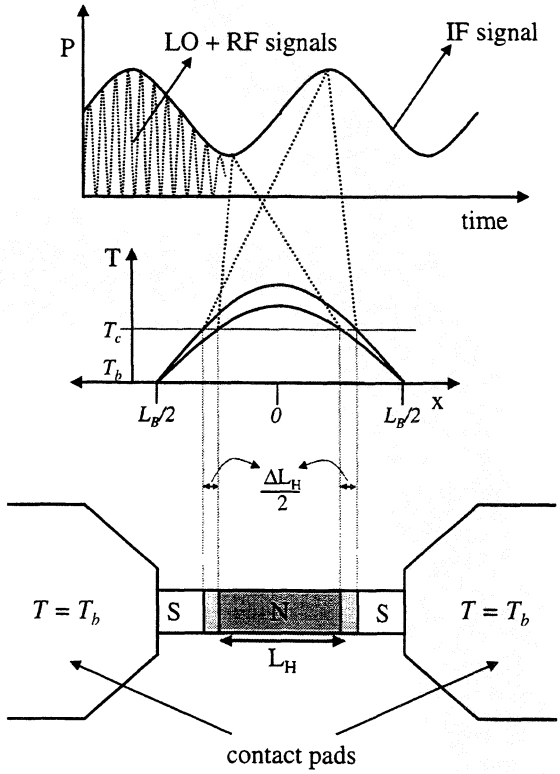

Fig. 1: Schematic representation of the electronic hot spot model. The microbridge is in a normal conducting state in those regions with $T>T_c$ (hot spot region). Beating of the absorbed RF power density at the intermediate frequency leads to a modulation of the length of the hot spot, and thus to a modulated resistance of the mixer.

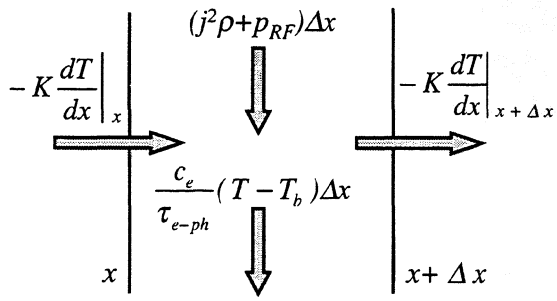

Fig. 2 : Heatflow diagram of a small segment Δx of the microbridge, from which the heat balance equations are derived.

them with the calculations. In Section IV we discuss the deviations between experiment and model.

II. Heat balance equations

If the critical current of the HEB is exceeded, the dc and RF power cause the formation of an electronic hot spot in the center of the otherwise superconducting microbridge [5,9]. With increasing power dissipation, the length of the hot spot, and thus the resistance, will increase and eventually asymptotically approach the normal state resistance of the bridge.

The heat flow inside a small segment Δx of the microbridge is depicted in Fig. 2. Joule heating occurs as a result of absorption of RF radiation and dc dissipation. Direct current dissipation only occurs inside the hot spot, whereas the RF radiation is absorbed homogeneously, because the RF frequency is assumed to be much larger than the gap frequency of the superconductor. The difference between the inflow and outflow of heat K(dT/dx), with K the thermal conductivity, at position x and x+Δx determines the magnitude of the diffusion term. Heat is transferred in the bulk from the electrons to the phonon bath. To parameterize which one of the two dominates for a microbridge with length L_B, it is convenient to introduce a so-called thermal healing length λ_{TH} given by [9]

$$\lambda_{TH} = \sqrt{\frac{K\tau_{e-ph}}{c_e}} = \sqrt{D\tau_{e-ph}} \,. \qquad [1]$$

Here, $\tau_{e\text{-}ph}$ is the electron-phonon energy scattering time, c_e is the electronic heat capacity and D is the electronic diffusion constant. If $\lambda_{TH}>L_B$, the HEB mixer is in the diffusion-cooled limit, in the opposite case it is phonon-cooled. Based on the heat flow diagram of

Fig. 2, we have the following heat-balance equations for a pumped microbridge with a normal state resistivity ρ_n, at a bath temperature T_B, and biased with a current density j:

$$-K\frac{d^2T}{dx^2}+\frac{c_e}{\tau_{e-ph}}(T-T_B)=j^2\rho_n+p_{RF} \qquad \text{(inside hot spot)} \qquad [2]$$

and

$$-K\frac{d^2T}{dx^2}+\frac{c_e}{\tau_{e-ph}}(T-T_B)=p_{RF} \qquad \text{(outside hot spot)} \qquad [3]$$

Here, p_{RF} is the RF power density (per unit volume). We solve these equations by requiring that, at the end of the microbridge, the electron temperature T equals the bath temperature T_B. In addition the electron temperature at the boundary of the hot spot equals the critical temperature of the microbridge T_c. Matching of K(dT/dx) at the hot spot boundary yields the following expression for the current as a function of the hot spot length L_H and p_{RF} :

$$j(L_H,p_{RF})=\sqrt{\frac{c_e}{\rho\tau_{e-ph}}\left[T_C-T_B-\frac{p_{RF}\tau_{e-ph}}{\rho_n}-\frac{\left[T_C-T_B-\frac{p_{RF}\tau_{e-ph}}{\rho_n}\right]\cosh\left[\frac{2L_H-L_B}{2\lambda_{TH}}\right]+\frac{p_{RF}\tau_{e-ph}}{\rho_n}}{\sinh\left[\frac{2L_H-L_B}{2\lambda_{TH}}\right]\tanh\left[\frac{L_H}{\lambda_{TH}}\right]}\right]} \qquad [4]$$

In the calculation, we have made a number of assumptions, which allow an analytical solution of the problem, but do not include the correct temperature dependence of the thermal conductivity and coupling strength between the electron and phonons. Therefore, a numerical calculation was performed [10].

First, in Eqs. 2 and 3, we have taken K independent of temperature, which is not true in reality. The thermal conductivity in the normal parts is described via the Wiedemann-Franz law, which states that the thermal conductivity is linearly dependent on the temperature. Also, in the superconducting parts K rapidly decreases with decreasing temperature due to the decreasing quasi-particle density. In our numerical approach we have used the following relations [11]

$$K=K_0\left(\frac{T}{T_c}\right) \qquad \text{(inside hot spot)} \qquad [5]$$

$$K=K_0\left(\frac{T}{T_c}\right)^3 \qquad \text{(outside hot spot)} \qquad [6]$$

where K_0 is the thermal conductivity at the critical temperature T_c. Note that Eq. 6 is an empirical relation, which is compatible with the microscopic theory in the relevant parameter range, but easier to use in the calculations.

Secondly, the cooling of hot-electrons is not linear in temperature, but is found to be proportional to T^4-T_B^4 [12]. Therefore, the second term in the heat-balance equations is replaced with

$$A\left(T^4 - T_B^4\right), \qquad [7]$$

where A is a constant and equal to $\sim 10^{10}$.

Finally, in the analytical model, the transition between the normal conducting parts and superconducting parts is sharply defined, by taking Eq. 2 and 3 in different domains. In reality, we suppose that the resistivity changes gradually from ρ_n to 0 over a certain length ΔL. To model this, we assume that we can express the change of the resistivity as a function of position near the interface by the Fermi-function

$$\rho(x) = \frac{\rho_N}{1 + e^{\frac{x - L_H}{\Delta L}}}. \qquad [8]$$

Since we calculate the temperature as a function of the position, it is convenient to use the following equivalent expression, by which we replace ρ_n of Eq. 2:

$$\rho(T) = \frac{\rho_n}{1 + e^{\frac{T - T_c}{\Delta T}}} \qquad [9]$$

A practical reason why Eq. 9 is used, is that it greatly simplifies the numerical procedure. Note that in the analysis we have assumed that an effective temperature can be attributed to each position in the microbridge, which implies a zero electron-electron interaction time.

III. I(V) characteristics of the pumped HEB

III.A Experimental

We measure the I(V) curves of the hot-electron bolometers as a function of applied RF power density and compare them with the results of the calculated I(V) curves based on the heat-balance equations. Details of the devices can be found in [13]. The bolometer is mounted in a fixed-tuned waveguide, designed for frequencies around 700 GHz and cooled down to 4.2 K. RF radiation is provided by a carcinotron with a doubler and coupled to the mixer via a mirror. The coupled RF power is regulated with an adjustable attenuator in the optical path. The measurements are performed at a frequency of exactly 700 GHz. The critical temperature of the microbridge is ~ 6 K, which corresponds to a

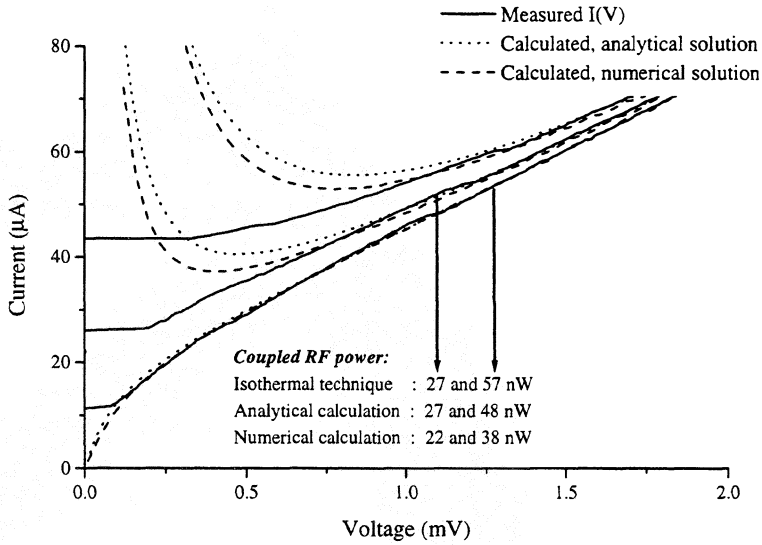

Fig. 3 : Measured and calculated I(V) curves. The solid curves are the measured characteristics, whereas the dotted and dashed curves are the calculated characteristics, resulting from the analytical and numerical solution of the problem, respectively

gap frequency of ~ 470 GHz. This justifies our assumption that the radiation of 700 GHz is absorbed homogeneously in the microbridge.

III. B Results

Fig. 3 shows three measured I(V) curves, together with the calculated ones. The data are obtained by using the dc bias-supply in bias-current mode. Note that this bias-supply, when operated in voltage-bias mode, does not allow measuring the regions of the I(V) curve with a negative differential resistance, due to oscillations. For clarity we only show the part of the I(V) which is recorded from high bias current to zero current. Therefore the hysteresis loop is not visible (the critical current of the unpumped curve is 120 μA). The measured data are corrected for a small series resistance of ~ 1 Ω, which originates from the electrical connection in the mixermount.

The measured curves are compared with the result of the analytical calculation, i.e. Eq. 4, and the numerical calculation. The parameters used for both calculations can be found in Table 1. They are determined by first optimizing the agreement between the unpumped curves. Fixing these values, we then calculate the pumped I(V) curves by adjusting only the absorbed RF power. We find a good agreement between model and measurement if we use 27 nW, 48 nW in the analytical calculations and 22 nW, 38 nW in the numerical calculations. Evidently, the numerical simulation predicts a somewhat

lower minimal current than the analytical result and is in somewhat better agreement with the measured curves.

We have also applied the isothermal technique at high current to determine the coupled RF power [14]. We find 27 nW and 57 nW, which is in reasonable agreement with the values calculated from the heat-balance equation as it should.

Table 1: *Parameters used for the calculated I(V) curves of figure 3.*

	D cm^2/s	c_e J/m^2K	$\tau_{e\text{-}ph}$ ns	T_B K	T_c K	L_B nm	λ_{TH} nm	K_0 W/mK	A W/m^3K^4
Analytical calculation	1.2	2800	1	4.3	5.9	300	350	-	-
Numerical calculation	-	-	-	4.3	5.9	300	-	0.32	$0.3\text{x}10^{10}$

IV. Discussion

A few comments can be made about the outcome of this comparison between measurements and calculations. As emphasized, the RF power densities, which follow from the conventional isothermal technique do hardly differ from those predicted by the EHS-model calculations. The isothermal technique is based on the lumped element approach, which implies that a change in dc power and RF power results in the same change in resistance of the device. At low bias voltage, where the length of the normal EHS is substantially smaller than the length of the microbridge, this is obviously incorrect. At large bias, however, the I(V) is quasi-Ohmic and the EHS boundaries reach to the end of the microbridge, so both dc power and RF power are dissipated along almost the full length of the microbridge. Therefore, the physical state of the microbridge closely corresponds to the state required in the isothermal technique.

It is obvious from Fig. 3, that at low bias, disagreement arises between the measured and calculated I(V) characteristics, in particular in the relevant experimentally accessible regime of positive differential resistance. In the EHS model the I(V) curve "bends up" with decreasing voltage, because the diffusion term in the heat balance equation is of growing importance with decreasing hot spot length (or voltage). The second derivative of the temperature profile increases with decreasing hot spot length. This implies, that as a counter balance, the dc power needed to sustain the hot spot, will decrease slower with decreasing hot spot length (non-Ohmic behavior) and eventually become almost constant. Consequently, the current and voltage become inversely proportional to each other and the differential resistance becomes negative [9].

Experimentally the measured minimum dc power to sustain the hot spot is found to be smaller than the predicted minimum dc power (see Fig. 3). This can only be reconciled within the model by assuming outflow of heat from the microbridge is less than assumed. Indeed, if the reduced thermal conductance in the superconducting parts is included better agreement is obtained. In addition, the interface is electrically conducting but constitutes a thermal boundary resistance for energies below the energy gap, which is the essence of Andreev reflection. This process is schematically represented in Fig. 4. Since there is no energy transfer during this process, heat will be partially trapped in the

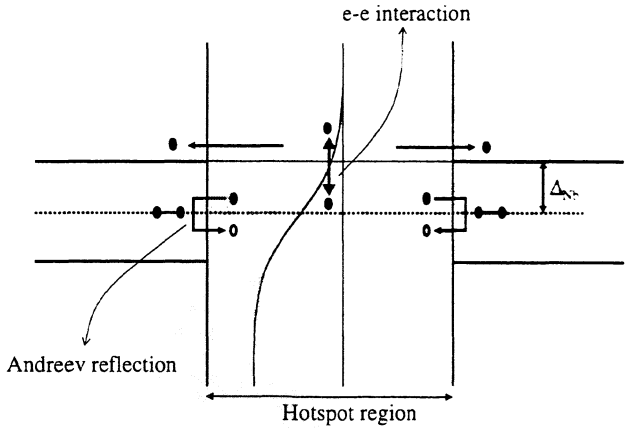

Fig. 4 : Representation of physical processes which are not included in the analysis, but are relevant in the heat transport. Andreev reflection occurs for energies below the gap energy of the superconductor and results in an additional heat transfer barrier at the N/S interface. Moreover, a non-thermal distibution function due to the finite electron-electron interaction time would require an energy dependent analysis of the heat tranport problem.

hot spot. Only those electrons with energies larger than the energy gap have a high probability to diffuse out into the superconducting parts.

Let us finally discuss the effect of a possible incomplete thermalization of the electron system. The electron-electron scattering time can be approximated by [15]

$$\tau_{in}^{-1} = 10^8 R_{sq} T \qquad [10]$$

with R_{sq} the square resistance of the material. This time, using Eq. 9, is ~ 50 ps in our samples at 6 K, which corresponds to an electronic thermalization length of 70 nm. In our analysis we have used as a starting assumption that an effective temperature can be attributed to each position in the microbridge, which implies an infinitely strong electron-electron interaction [5]. The effect of a having non-thermal distribution function is beyond the scope of our current investigations. However, incomplete thermalization is an important issue for the sensitivity of the bolometer, and might cause a reduced mixer conversion gain [16].

V. Conclusions

In conclusion, we have compared I(V) curves of Nb diffusion-cooled HEB pumped above the gap frequency with the electronic hot spot model. We find an excellent agreement at high voltage, whereas deviations at low voltage can be accounted for in a plausible way by pointing out certain simplifications made in the model: the reduced thermal conductance in the superconducting parts of the microbridge and the existence of a thermal barrier as implied by the process of Andreev reflection.

Acknowledgements

Useful discussions with M. Dröge, H. W. Hoogstraten, H. Merkel, B. J. van Wees, and W. F. M. Ganzevles are acknowledged. This work is supported by the European Space Agency (ESA) under Contract No. 11738/95/NL/PB and by the Nederlandse Organisatie voor Wetenschappelijk Onderzoek (NWO) through the Stichting voor Technische Wetenschappen (STW).

References

[1] B. S. Karasik and A. I. Elantiev, Appl. Phys. Lett. 68, 853 (1996).
[2] D.E. Prober, App. Phys. Lett. 62, 2119 (1993).
[3] D. Wilms Floet, J. J. A. Baselmans, T.M. Klapwijk, and J.R. Gao, Appl. Phys. Lett. 73, 2826 (1998).
[4] D. Wilms Floet, J.J.A. Baselmans, J.R. Gao, and T.M. Klawpijk, Proc. 9th Int. Symp. Space THz Technology, Jet Propulsion Laboratory, Pasadena, March 17-19 1998, pp 63-72.
[5] D. Wilms Floet, E. Miedema, T. M. Klapwijk, and J. R. Gao, Appl. Phys. Lett. 74, 433 (1999).
[6] H. F. Merkel, E. L. Kollberg, K. S. Yngvesson, Proc. 9th Int. Symp. Space THz Technology, Jet Propulsion Laboratory, Pasadena, 17-19 March 1998, pp 81-97.
[7] A. Skalare and W. R. McGrath, submitted to the 1998 Applied Superconductivity Conference, Palm Desert, USA (1998).
[8] H. Araújo and G. J. White, submitted to the 1998 Applied Superconductivity Conference, Palm Desert, USA (1998).
[9] The critical current density of the microbridge can be much larger than the minimum current density that is needed to sustain the hot spot. This is the reason why, in a current bias situation, a strong hysteresis effect in the I(V) curve is observed; see also W. J. Skocpol, M. R. Beasley, and M. Tinkham, J. Appl. Phys. 45, 4054 (1974).
[10] Numerical procedure and programm by M. Dröge and H. W. Hoogstraten.
[11] Superconductivity Vol.1, edited by R. D. Parks, Marcel Dekker Inc, New York (1969).
[12] E.M. Gershenzon, G.N. Gol'tsman, A. I. Elant'ev, B. S. Karasik, and S. E. Potoskuev, Sov. J. Low Temp. Phys. 14, 414 (1988).
[13] D. Wilms Floet, J. R. Gao, T. M. Klapwijk, W. F. M. Ganzevles, G. de Lange, and P. A. J. de Korte, presented at the 10th Int. Symp. Space THz Technology, University of Virginia, Charlottesville, March 16-18 (1999).
[14] H. Ekström, B. S. Karasik, E. Kollberg, and K. S. Yngvesson, IEEE Trans. Microwave Theory Techn. 43, 938 (1995).
[15] P. Santhanam and D. E. Prober, Phys. Rev. B 29 3733 (1984).
[16] A. D. Semenov, G. N. Gol'tsmann, submitted to the 1998 Applied Superconductivity Conference, Palm Desert, USA (1998).